

Different routes to chaos via strange nonchaotic attractor in a quasiperiodically forced system

A. Venkatesan and M. Lakshmanan
*Centre for Nonlinear dynamics,
Department of Physics,
Bharathidasan University,
Tiruchirapalli 620 024, INDIA*

Abstract

This paper focusses attention on the strange nonchaotic attractors (SNA) of a quasiperiodically forced dynamical system. Several routes, including the standard ones by which the appearance of strange nonchaotic attractors takes place, are shown to be realizable in the same model over a two parameters (f - ϵ) domain of the system. In particular, the transition through torus doubling to chaos via SNA, torus breaking to chaos via SNA and period doubling bifurcations of fractal torus are demonstrated with the aid of the two parameter (f - ϵ) phase diagram. More interestingly, in order to approach the strange nonchaotic attractor, the existence of several new bifurcations on the torus corresponding to the novel phenomenon of torus bubbling are described. Particularly, we point out the new routes to chaos, namely, (1) two frequency quasiperiodicity \rightarrow torus doubling \rightarrow torus merging followed by the gradual fractalization of torus to chaos, (2) two frequency quasiperiodicity \rightarrow torus doubling \rightarrow wrinkling \rightarrow SNA \rightarrow chaos \rightarrow SNA \rightarrow wrinkling \rightarrow inverse torus doubling \rightarrow torus \rightarrow torus bubbles followed by the onset of torus breaking to chaos via SNA or followed by the onset of torus doubling route to chaos via SNA. The existence of the strange nonchaotic attractor is confirmed by calculating several characterizing quantities such as Lyapunov exponents, winding numbers, power spectral measures and dimensions. The mechanism behind the various bifurcations are also briefly discussed.

PACS number(s): 05.45.+b

I. INTRODUCTION

In nonlinear dynamical systems strange nonchaotic attractors (SNA) are considered as complicated structures in phase space, which is a property usually associated with chaotic attractors. The pioneering work of Grebogi et al. [1] revealed that there are some possibilities of strange attractors in certain types of dynamical systems which are not chaotic. These strange attractors are strange in the spirit that geometrically they are strange (fractal dimensional) objects in phase space. On the other hand, they would not exhibit sensitivity to initial conditions (for example, Lyapunov exponents are negative), and hence are not chaotic. These strange nonchaotic attractors can arise in physically relevant situations such as quasiperiodically forced pendulum [2-4], quantum particles in quasiperiodic potentials [5], biological oscillators [6], Duffing type oscillators [7-10], velocity dependent oscillators [11], electronic circuits [12,13] and in certain maps [14-22]. Also these exotic attractors were confirmed by an experiment consisting of a quasiperiodically forced, buckled magnetoelastic ribbon [23], in analog simulations of a multistable potential [24] and in a neon glow discharge experiment [25].

While the existence of strange nonchaotic attractors has been firmly established, a question that remains interesting is what are the possible routes by which they arise and ultimately become chaotic, and how do these attractors are born in a system (mechanism). Several routes have been identified in recent times and for a few of them typical mechanisms have also been found for the creation of SNA. The major routes by which the SNA appear, may be broadly classified as follows.

1. Ding et al. route [6]: two frequency quasiperiodicity \rightarrow three frequency quasiperiodicity \rightarrow strange nonchaotic attractor \rightarrow chaos.

2. Kapitaniak et al. route [10]: two frequency quasiperiodicity \rightarrow strange nonchaotic attractor \rightarrow three frequency quasiperiodicity \rightarrow chaos.

3. Heagy and Hammel route [14]: two frequency quasiperiodicity \rightarrow torus doubling \rightarrow wrinkling \rightarrow strange nonchaotic attractors \rightarrow chaos.

4. Feudal et al. route [17]: two frequency quasiperiodicity \rightarrow wrinkling \rightarrow strange nonchaotic attractors \rightarrow chaos.

5. Yalencinkaya and Lai route [9]: two frequency quasiperiodicity \rightarrow strange nonchaotic attractor (on-off intermittency type attractor) \rightarrow chaos.

6. Venkatesan and Lakshmanan route [11]: two frequency quasiperiodicity \rightarrow torus doubling \rightarrow torus merging \rightarrow wrinkling \rightarrow strange nonchaotic attractor \rightarrow chaos.

7. Kapitaniak and Chua route [13]: two frequency quasiperiodicity \rightarrow strange nonchaotic trajectories on torus \rightarrow chaos.

8. Nishikawa and Kaneko route [21]: two frequency quasiperiodicity \rightarrow strange nonchaotic attractors \rightarrow chaos.

Different mechanisms have been identified for some of the above routes. In particular, it has been shown that the birth of SNA in the Heagy and Hammel [14] route is due to the collision between a period doubled torus and its unstable torus. Feudal et al.[17] explained in their route that the SNA also appears a result of a collision of stable and unstable torus in a dense set of points. However, Nishikawa and Kaneko [21] discussed in their route that the SNA emerges without interaction of stable and unstable torus. Moreover, the loss of transverse stability of the torus can also lead to the birth of SNA, as in the case of

the Yalencinkaya and Lai route [9] above. For other routes as far as our knowledge goes mechanisms have not yet been found.

Also, most studies of strange nonchaotic attractors have focussed on their characterization using the spectral properties[2,5], geometrical properties[6], local divergence of trajectories[10], phase sensitivity and rational bifurcations [15-18], and functional maps and invariant curves [20-21].

In this paper, we demonstrate the existence of at least five different routes to chaos via strange nonchaotic attractors in a single dynamical system namely a quasiperiodically forced velocity dependent nonpolynomial oscillator system over a two parameters (f - ϵ) space. To start with the birth of the strange nonchaotic attractors associated with two important routes, namely, (i) torus breaking and (ii) torus doubling, have been studied in our model. In low dimensions, Bier and Bountis have shown that a dynamical system that undergoes one or more period doublings need not complete the entire infinite Feigenbaum cascade, but it may be possible to have only a finite number of period doublings, followed by for example undoublings or other bifurcations [28]. The possibility of such a novel remerging bifurcation phenomenon of the torus doubling sequence in the quasiperiodically forced system has not yet been reported. Since the system that we consider possesses more than one control parameter and remains invariant under the reflection symmetry, the remergence is likely to occur as in the case of low dimensional systems [28,29]. To confirm such a possibility, our numerical studies show that in some regions of the (f - ϵ) parameter space, torus doubled orbit emerges and remerges from a single torus orbit at two different parameter values of ϵ to form a torus bubble. Such a remerging bifurcation can lead to tame the growth of the torus doubled trees and the development of the associated universal route to chaos further. However, the nature of remerging torus doubled trees or more specifically torus bubbling, ensures the existence of different routes for the creation of SNA when the full range of parameters are taken into account. To illustrate these possibilities in our system, we enumerate two new types of routes as: (1) two frequency quasiperiodicity \rightarrow torus doubling \rightarrow torus merging followed by the gradual fractalization of torus to chaos [11], (2) two frequency quasiperiodicity \rightarrow torus doubling \rightarrow wrinkling \rightarrow SNA \rightarrow chaos \rightarrow SNA \rightarrow wrinkling \rightarrow inverse torus doubling \rightarrow torus \rightarrow torus bubbles followed by the onset of torus breaking to chaos via SNA or followed by the onset of torus doubling route to chaos via strange nonchaotic attractor. Finally, we also show the occurrence of period doubling bifurcations of the destroyed torus (strange nonchaotic attractor) in our model.

This paper is organised as follows. Sec. 2 describes the system and the salient features of its dynamics. Sec. 3 describes some of the characterizing quantities of strange nonchaotic attractors in comparison with chaotic attractors such as Lyapunov exponents, winding number, power spectral analysis and dimensions. These quantities have been used to distinguish between quasiperiodic, strange nonchaotic and chaotic attractors. The birth of strange nonchaotic attractors from the transitions of the two frequency quasiperiodic attractors are observed in the five different routes mentioned above in sec. 4. The first one is that of torus breaking to chaos via SNA. The second one is through torus bubbling followed by the gradual fractalization to chaos. The third route is the transition from torus doubling to chaos via strange nonchaotic attractor. The next one we notice is the possibility of torus doubling to chaos via SNA followed by the inversely advancing type of torus. The last one we observe is the period doubling bifurcation of the destroyed torus. Finally, in sec. 5 we

summarize our results.

II. QUASIPERIODICALLY FORCED VELOCITY DEPENDENT SYSTEM

Let us consider briefly the dynamics of a damped and driven rotating parabola system and discuss some of its general properties as reported in ref.[11].

A mechanical model describing the motion of a freely sliding particle of unit mass on a parabolic wire ($z=\sqrt{\lambda}x^2$) rotating with a constant angular velocity Ω ($\Omega^2 = \Omega_o^2 = -\omega_o^2 + g\sqrt{\lambda}$) and g is the acceleration due to gravity) can be associated with a velocity dependent Lagrangian [27]

$$L = \frac{1}{2} [(1 + \lambda x^2)\dot{x}^2 - \omega_o^2 x^2]. \quad (1)$$

Here overdot stands for a derivative with respect to time. The corresponding equation of motion is

$$(1 + \lambda x^2)\ddot{x} + \lambda x \dot{x}^2 + \omega_o^2 x = 0, \quad (2)$$

When $\omega_o^2 > 0$, Eq.(2) can be integrated in terms of elliptic integrals. Interesting bifurcations and different routes to chaos occur in the above model when the system is acted upon by additional damping and external forcing [11]. In this case, Eq.(2) gets modified to

$$(1 + \lambda x^2)\ddot{x} + \lambda x \dot{x}^2 + \omega_o^2 x + \alpha \dot{x} = f \cos \omega t. \quad (3)$$

The familiar period doubling bifurcations, preceded by a symmetry breaking bifurcation, intermittency and antimonotonicity have been identified by us earlier in ref [11].

Another interesting physical situation is the case in which there is an additional parametric modulation in the angular velocity,

$$\Omega = \Omega_o(1 + \epsilon \cos \omega_p t),$$

so that we can replace $\omega_o^2 = g\sqrt{\lambda} - \Omega_o^2$ in Eqs. (1)-(3) by $g\sqrt{\lambda} - \Omega^2 = \omega_o^2 - \Omega_o^2[2\epsilon \cos \omega_p t + 0.5\epsilon^2(1 + \cos 2\omega_p t)]$. Then the equation of motion becomes (see for example p.351 in ref. [27] and also ref. [11])

$$(1 + \lambda x^2)\ddot{x} + \lambda x \dot{x}^2 + \omega_o^2 x - \Omega_o^2[2\epsilon \cos \omega_p t + 0.5\epsilon^2(1 + \cos 2\omega_p t)]x + \alpha \dot{x} = f \cos \omega_e t, \quad (4)$$

where ϵ is a small parameter.

We have already noted an interesting new quasiperiodic route to chaos, namely two frequency quasiperiodicity \rightarrow torus doubling \rightarrow torus merging \rightarrow wrinkling \rightarrow strange non-chaotic attractor \rightarrow chaos in the system (4) in ref.[11]. In this paper we make a detailed study of this and many other quasiperiodic routes to chaos which can occur in this model in a range of f - ϵ parameter values and compare them. For our analysis we rewrite the system (4) as

$$\begin{aligned}
\dot{x} &= y, \\
\dot{y} &= \left[\frac{-\lambda xy^2 - \{\omega_o^2 - \Omega_o^2[2\epsilon \cos \phi + 0.5\epsilon^2(1 + \cos 2\phi)]\}x - \alpha y + f \cos \theta}{(1 + \lambda x^2)} \right], \\
\dot{\phi} &= \omega_p, \\
\dot{\theta} &= \omega_e.
\end{aligned} \tag{5}$$

We note that the system (5) remains invariant under the reflection symmetry $(x, y, f) \rightarrow (-x, -y, -f)$, (or equivalently (4) under the transformation $(x, f) \rightarrow (-x, -f)$). In analogy with low dimensional systems involving more than one control parameter when period bubbles occur [28], one may expect reemergence of torus doubling sequences to occur in this model, which we indeed show to be true in the following.

III. CHARACTERIZATION OF THE QUASIPERIODIC, STRANGE NONCHAOTIC AND CHAOTIC ATTRACTORS

There are several quantities to characterize the attractors, which are useful to distinguish strange nonchaotic from chaotic and quasiperiodic attractors. We briefly review some of them which we will use in our study.

A. The Lyapunov exponents

For the system (5), there are two Lyapunov exponents that are trivial in the sense that they are identically zero by virtue of the two excitation frequencies. Let the Lyapunov exponents λ_i be ordered by their values, $\lambda_1 \geq \lambda_2 \geq \lambda_3 \geq \lambda_4$. We then have the following possibilities: (1) two frequency quasiperiodic attractors, $\lambda_1 = \lambda_2 = 0 > \lambda_3, \lambda_4$, (2) three frequency quasiperiodic attractors, $\lambda_1 = \lambda_2 = \lambda_3 = 0 > \lambda_4$, (3) strange chaotic attractors, atleast $\lambda_1 > 0$ and (4) strange nonchaotic attractors, the same as two frequency quasiperiodic attractors.

B. Winding number

The winding number for the orbit of Eq.(5) is defined by the limit

$$W = \lim_{t \rightarrow \infty} \left\{ \frac{(\alpha(t) - \alpha(t_o))}{t} \right\}, \tag{6}$$

where $(x, \dot{x}) = (r \cos \alpha, r \sin \alpha)$. For the two frequency quasiperiodic attractors, the winding number satisfies

$$W = \frac{l}{n}\omega_p + \frac{m}{n}\omega_e, \tag{7}$$

where l, m , and n are integers. Combining the winding number and the Lyapunov exponents, we can distinguish the strange nonchaotic attractors from the other nonchaotic attractors as noted in Table I.

C. Power spectrum analysis

To quantify the changes in the power spectrum (obtained using Fast Fourier Transform (FFT) technique) one can compute the so called spectral distribution function $N(\sigma)$, defined to be the number of peaks in the Fourier amplitude spectrum larger than some value say σ . Scaling relations have been predicted for $N(\sigma)$ in the case of two, three frequency quasiperiodic and strange nonchaotic attractors. These scaling relations are $N(\sigma) \sim \ln \frac{1}{\sigma}$, $N(\sigma) \sim \ln^2 \sigma$, and $N(\sigma) \sim \sigma^{-\beta}$ respectively corresponding to two, three frequency quasiperiodic and strange nonchaotic attractors. In the Romeiras and Ott [2] studies, the power law exponent was found empirically to lie within the range $1 < \beta < 2$ for the strange nonchaotic attractor. Thus the above characterizations allow us to distinguish the strange nonchaotic attractor from other nonchaotic attractors as seen in Table I.

D. Dimensions

To quantify geometric properties of attractors, several methods have been used to compute the dimension of the attractors. Among them, what we have used is the correlation dimension (introduced by Grassberger and Procaccia [26]) which may be computed from the correlation function $C(R)$ defined as

$$C(R) = \lim_{N \rightarrow \infty} \left[\frac{1}{N^2} \sum_{i,j=1}^N H(R - |x_i - x_j|) \right],$$

where x_i and x_j are points on the attractor, $H(y)$ is the Heaviside function (1 if $y \geq 0$ and 0 if $y < 0$), N is the number of points randomly chosen from the entire data set. The Heaviside function simply counts the number of points within the radius R of the point denoted by x_i and $C(R)$ gives the average fraction of points. Now the correlation dimension is defined by the variations of $C(R)$ with R :

$$C(R) \sim R^d \quad \text{as} \quad R \rightarrow 0.$$

Therefore the correlation dimension (d) is the slope of a graph of $\log C(R)$ versus $\log R$. Once one obtains the dimensions of the attractors, it will be easy to quantify strange property of the attractors as seen in Table I.

IV. DIFFERENT ROUTES TO CHAOS VIA STRANGE NONCHAOTIC ATTRACTORS

Now we consider the combined effect of both the external and parametric forcings in Eq. (5). To be concrete, we consider the dynamics of (5) and numerically integrate it using the fourth order Runge-Kutta algorithm with adaptive step size with the values of the parameters fixed at $\omega_o^2=0.25$, $\lambda=0.5$, $\alpha=0.2$, $\Omega_o^2=6.7$, $\omega_p=1.0$ and $\omega_e=0.991$. Various characteristic quantities such as the winding numbers, Lyapunov exponents, power spectral measures and dimensions as discussed in the previous section have been used to distinguish quasiperiodic, strange nonchaotic and chaotic attractors. Further to identify the different

attractors, the dynamical transitions are traced out by two scanning procedures: (i) varying f at a fixed ϵ and (ii) varying ϵ at a fixed f . The resulting phase diagram in the $(f-\epsilon)$ parameter space is shown in Fig.1. The various features indicated in the phase diagram are summarised and the dynamical transitions are elucidated in the following.

A. Torus breaking bifurcations and the birth of strange nonchaotic attractors

For low f and low ϵ values, the system exhibits two frequency quasiperiodic oscillations denoted by 1T in Fig. 1. When the value of ϵ exceeds a certain critical value for a fixed low f , a transition from two frequency quasiperiodic (1T) to chaotic attractor(C) via strange nonchaotic attractor (S) occurs on increasing ϵ . For example, we fix the strength of the external forcing parameter value as $f=0.302$ and vary the modulation parameter ϵ . For $\epsilon=0.03$, Fig. 2a of the attractor has smooth branches and this indicates that the system is in a two frequency quasiperiodic state. As ϵ increases, the branches in the Fig. 2b start to wrinkle (W1). As ϵ increases further, the attractor becomes extremely wrinkled and has several sharp bends. The sharp bends appear to become actual discontinuities at $\epsilon=0.0419$ and ultimately result in fractal phenomenon. Such a phenomenon is essentially the result of the collision of stable and unstable torus in a dense set of points as was shown by Feudel et al. in their route to chaos via SNA [17]. At such values, the nature of the attractor is strange (Fig. 2c) eventhough the largest Lyapunov exponent in Fig. 3 remains negative. For this attractor, the correlation dimension is 1.33 while the Fourier amplitude scaling constant (σ) is 1.54. Winding number W does not satisfy the relation (7) for this attractor. Hence, these studies confirm further that the attractor shown in Fig. 2c is strange nonchaotic. As ϵ increases further, an attractor visibly similar to Fig. 2c appears (see Fig 2d for $f=0.042$). However, it has a positive Lyapunov exponent and hence it corresponds to a chaotic attractor.

B. Remerging torus doubling bifurcations: torus bubble and its consequences

1. Torus bubbling

On increasing the forcing parameter f further, $0.305 < f < 0.325$, the fascinating novel phenomenon of torus bubble appears within a range of values of ϵ . Within this range of f , on increasing the value of ϵ along the same line, the onset of chaos is realised via strange nonchaotic attractor. To be more specific, the parameter f is fixed at 0.32 and ϵ is varied. For $\epsilon=0.03$, the attractor is a two frequency quasiperiodic attractor (Figs. 4a & 5a). As ϵ is increased to $\epsilon=0.0317$, the attractor undergoes a torus doubling bifurcation (Figs. 4b & 5b). The corresponding period doubled torus attractor is denoted as 2T in Fig. 1. We note from Figs. 4 and 5 that the two strands in the (x, ϕ) projection become four strands when torus doubling bifurcation occurs. When we compute ϕ modulo 4π instead of 2π during integration, we notice from Figs. 5 that the two bifurcated strands of length 2π are actually a single strand of length 4π . As a result, it can be concluded that the torus doubling is nonetheless a length doubling bifurcation. Further, it may be noted that this bifurcation is geometrically very similar to that of period doubling bifurcation in the three dimensional

flows. One then expects as ϵ is increased further that the doubled attractor has to continue the doubling sequence as in the case of period doubling phenomenon. Instead, in the present case, interestingly the strands of the length doubled attractor begin to merge into that of a single attractor at $\epsilon=0.0353$ as shown in Fig 6a, leading to the formation of a torus bubble (see Fig. 1), reminiscent of period bubbles in low dimensional systems [28,29]. On further increase of the value of ϵ , the transition from two frequency quasiperiodicity to chaos via strange nonchaotic attractor takes place due to torus breaking bifurcations as discussed in section 4.A (see Figs 6 b,c,& d and Fig. 7).

It has been argued in the case of period bubbling in low dimensional systems [28] that the cause of formation of the period bubbles is essentially due to the presence of reflection symmetry combined with more than one control parameter present in the system. It appears that similar argument holds good for the case of higher dimensions for the formation of torus bubbles.

2. Formation of multibubbles

As the forcing parameter f is increased further in the region $0.325 < f < 0.332$, the evolution of attractor undergoes the following transition to chaos, wherein more than one bubble is formed on increasing the value of ϵ : two frequency quasiperiodicity \rightarrow torus doubling \rightarrow wrinkling \rightarrow inverse torus doubling (doubled torus) \rightarrow merged torus \rightarrow torus bubble \rightarrow merged torus \rightarrow wrinkling \rightarrow SNA \rightarrow chaos. To illustrate this possibility, let us fix the forcing parameter value as $f=0.328$ and vary the ϵ value. For $\epsilon=0.03$ the attractor is two frequency quasiperiodic. As ϵ is increased to $\epsilon=0.0313$, the attractor undergoes to torus doubling bifurcation. The doubled attractor begins to wrinkle when the ϵ value is increased. However, this wrinkled attractor appears to become again a torus doubled attractor, instead of approaching the SNA while the ϵ value is increased further. This doubled attractor merges into a single torus through inverse bifurcation on increasing the value of ϵ . The merged torus again forms a torus bubble and then finally transits to chaos via wrinkling and SNA as the value of the ϵ is increased further.

On increasing the forcing parameter f further, $0.332 < f < 0.335$, the transition from two frequency quasiperiodicity to chaos via SNA takes place through the following route, wherein more than two bubbles are formed as ϵ increases: two frequency quasiperiodicity \rightarrow torus doubling \rightarrow wrinkling \rightarrow inverse torus doubling \rightarrow merged torus \rightarrow torus bubble \rightarrow torus \rightarrow torus bubble \rightarrow torus \rightarrow wrinkling \rightarrow SNA \rightarrow chaos.

C. Strange nonchaotic and chaotic attractors within and outside the main torus bubble

On further increase of f , $f > 0.335$, inside the main torus bubble we observe interesting possibilities of strange nonchaotic and chaotic attractors via wrinkling as ϵ increases. Then two interesting possibilities arise inside the main bubble. The dynamics outside the main bubble more or less follows the previous case 3B. The details are as follows.

1. SNA within the main torus bubble

In a narrow region of f , $0.335 < f < 0.339$, the SNA undergoes an inverse bifurcation scheme leading to two frequency quasiperiodic attractor as ϵ increases through the following route: two frequency quasiperiodicity \rightarrow torus doubling \rightarrow wrinkling \rightarrow SNA \rightarrow wrinkling \rightarrow inverse torus doubling (doubled torus) \rightarrow merged torus. For example, the forcing parameter f is fixed at $f=0.337$ and ϵ is varied. For $\epsilon=0.03$ the attractor is a two frequency quasiperiodic one (Fig. 8a). As ϵ is increased to $\epsilon=0.031$, the attractor undergoes a torus doubling bifurcation (as seen in Fig. 8b). In lower dimensional systems, the period doubling occurs in an infinite sequence until the accumulation point is reached, beyond which chaotic behaviour appears. However, with tori, in the present case, the truncation of the torus doubling begins when the two strands become extremely wrinkled (W2) when the ϵ value is increased, as shown in Fig. 8c. These strands lose their continuity as well as smoothness and become strange at $\epsilon = 0.0339$. At such values, the attractor possesses geometrically strange property but does not obey the sensitivity to the initial conditions (the maximal Lyapunov exponent is negative as seen in Fig. 9) and so it is named as strange nonchaotic attractor (Fig. 8d). The emergence of such SNA is due to the collision of stable doubled torus and its unstable parent as was shown by Heagy and Hammel[14] in their route. Interestingly the SNA (Fig. 8e), instead of approaching a chaotic attractor as the ϵ value increases, becomes wrinkled (Fig. 8f) and then torus doubled attractor (Fig. 8g). The doubled attractor again merges into a single torus (Fig. 8h) on further increasing the value of ϵ .

2. Chaotic attractor within the main torus bubble

In a rather large region of f , $f > 0.339$, the SNA as formed above transits into chaotic attractor on increasing the value of ϵ further through the following route: two frequency quasiperiodicity \rightarrow torus doubling \rightarrow wrinkling \rightarrow SNA \rightarrow chaos \rightarrow SNA \rightarrow wrinkling \rightarrow inverse torus doubling (doubled torus) \rightarrow merged torus. To illustrate this possibility, let us choose the parameter $f=0.342$, and vary the value of ϵ . For $\epsilon=0.03$ the attractor is a two frequency quasiperiodic attractor (Fig. 10a). As ϵ is increased to $\epsilon=0.0309$, the attractor undergoes a torus doubling bifurcation (Fig. 10b). As ϵ is increased further the strands of the doubled attractor begin to wrinkle (W2), as shown in Fig. 10c. The formation of sharp bends in the strand of the attractor is now clear as ϵ is increased further. These bends tend to become actual discontinuities at $\epsilon = 0.0337$, as shown in Fig. 10d. The emergence of such dicontinuites on the torus is due to the collision of stable doubled torus and its unstable parent which is similar to the one found by Heagy and Hammel [14]. At such values, the attractor loses smoothness and becomes "strange". The attractor shown in Fig. 10d is nothing but strange nonchaotic as the maximum Lyapunov exponent works out to be $\lambda = -0.01213$ (Fig. 11). Further the correlation dimension is 1.49, the scaling constant (σ) is 1.38 and winding number W does not satisfy the relation (7) for this attractor. Hence, these characteristic studies confirm further that the attractor shown in Fig. 10d is strange but nonchaotic. On increasing ϵ value further, for a narrow range of ϵ values, period doubling bifurcation of SNA is also noticed, which will be discussed in detail in the following subsection. On further increase of the value of ϵ to 0.034, we find the emergence of a chaotic attractor (Fig. 10e), which though visibly similar to the nonchaotic strange attractor Fig.

10d, has a positive Lyapunov exponent (see Fig. 11). The chaotic attractor again becomes SNA when ϵ is further increased (Fig. 10f). As the value of ϵ is still increased, the SNA becomes torus doubled attractor (Fig. 10g) via wrinkling. This doubled attractor then merges into a single torus (Fig. 10h) when the value ϵ is continuously increased.

3. Dynamics outside the main torus bubble

Two further interesting transitions exist outside of the main torus bubble, namely (i) torus breaking to chaos via SNA and (ii) torus doubling to chaos via SNA. The details are as follows.

In a narrow region of f , $0.335 < f < 0.345$, the transition from two frequency quasiperiodicity to chaos via SNA takes place outside the main bubble through the following route as ϵ increases beyond $\epsilon = 0.0361$: torus \rightarrow torus bubble \rightarrow torus \rightarrow torus bubble \rightarrow torus \rightarrow wrinkling \rightarrow SNA \rightarrow chaos. However in the region of f , $0.345 < f < 0.352$, one also observes a transition from a wrinkled two torus (W2) to a wrinkled one torus (W1).

Further increase of the value of f beyond 0.352, for ϵ values greater than 0.0362, introduces yet another kind of transitions beyond the main bubble as torus \rightarrow torus doubling \rightarrow wrinkling \rightarrow inverse torus doubling \rightarrow merged torus \rightarrow torus doubling \rightarrow wrinkling \rightarrow strange nonchaotic attractor \rightarrow chaos.

D. Period doubling bifurcations of destroyed torus (SNA) within the main torus bubble

In the previous subsections, we have seen that the period doubling bifurcation of torus has been truncated by the destruction of the torus leading to the emergence of strange nonchaotic attractor in certain regions of the $(f-\epsilon)$ parameter space. However, we observe in the present system that in some cross sections of the $(f-\epsilon)$ parameter space, the period doubling bifurcation phenomena still persists in the destroyed torus, even though the actual doubling sequence of the torus has been terminated. Such a route has also been recently observed in coupled Duffing oscillators [8] and in certain maps [22]. The doubling of destroyed torus has been observed in the present model in a rather long range of f , $0.338 < f < 0.358$ and for a narrow range of ϵ values denoted by S2 in Fig.1. For example, let us choose $f=0.345$ and vary the value of ϵ . For $\epsilon=0.03$, the attractor is a two frequency quasiperiodic torus (Fig. 12a). As ϵ is increased to $\epsilon=0.0305$, the system undergoes torus doubling bifurcations (Fig. 12b). On increase of the value of ϵ further, the attractor begins to wrinkle and finally ends up with fractal nature (SNA) (Fig. 12c). On further increase of the value of ϵ , the fractal torus undergoes doubling bifurcation (Fig. 12d). If the parameter ϵ is still increased, the doubled fractal torus merges into a single fractal torus and finally transits into the chaotic attractor.

V. CONCLUSION

In this paper, we considered the dynamics of the specific example of the quasiperiodically forced velocity dependent nonpolynomial oscillator system (5) which illustrates many of the

typical routes to chaos via strange nonchaotic attractors. It was found that the first two of these routes can be realized in the following ways.

- two frequency quasiperiodicity \rightarrow torus doubling \rightarrow wrinkling \rightarrow strange nonchaotic attractor \rightarrow chaos. Here, the birth of SNA is due to the collision of stable doubled orbit and its unstable parent torus [14].
- two frequency quasiperiodicity \rightarrow wrinkling \rightarrow strange nonchaotic attractor \rightarrow chaos. In this case, the emergence of SNA is essentially the result of interaction of stable and unstable torus in a dense set of points [17].

More interestingly, we have pointed out the novel possibility of the torus bubbling. That is torus doubling bifurcations in dynamical systems can under suitable circumstances form finite sequence which ‘merge’ in some cross sections of the parameters space, inhibiting the onset of torus doubling route to chaos. Such remerging bifurcations having finite number of ‘bubbles’ occur only within some range of the parameters values. An important consequence is of such remerging is that the orbits become again stable and relatively large regions reappear around them, where the motion is regular and predictable. To illustrate such remerging torus doubling bifurcations, in our present study, we have shown two more routes:

- two frequency quasiperiodicity \rightarrow torus doubling \rightarrow torus merging followed by the gradual fractalization of torus to chaos via SNA
- two frequency quasiperiodicity \rightarrow torus doubling \rightarrow wrinkling \rightarrow SNA \rightarrow chaos \rightarrow SNA \rightarrow wrinkling \rightarrow inverse torus doubling \rightarrow torus \rightarrow torus bubbles followed by the onset of torus breaking to chaos via SNA or followed by the onset of torus doubling route to chaos via SNA.

From these routes, it can be concluded that prior to standard routes for transition to strange nonchaotic attractor, the possibilities of several bifurcations on the torus can be realised.

Finally, the period doubling bifurcations of the destroyed torus have also been observed in our model in a narrow region of the $(f - \epsilon)$ parameter space:

- two frequency quasiperiodicity \rightarrow torus doubling \rightarrow wrinkling \rightarrow destroyed torus \rightarrow period doubling of destroyed torus \rightarrow merged destroyed torus \rightarrow chaos.

VI. ACKNOWLEDGEMENTS

This work forms part of a Department of Science and Technology, Government of India research project. Also one of the authors (A.V) wishes to acknowledge the Council of Scientific and Industrial Research, Government of India, for providing a Senior Research Fellowship.

REFERENCES

- [1] C. Grebogi, E. Ott, S. Pelikan and J.A. Yorke, *Physica* 13D, 261 (1984).
- [2] F.J. Romeiras and E. Ott, *Phys. Rev*A35, 4404 (1987); F.J. Romeiras, A. Bonderson, E. Ott, T.M. Anderson jr. and C. Grebogi, *Physica* 26D, 277 (1987).
- [3] Y.C. Lai, *Phys. Rev* E53, 57 (1996)
- [4] Y. C. Lai, U. Feudel and C. Grebogi, *Phys. Rev* E54, 6114 (1996).
- [5] A. Bonderson, E. Ott and T. M. Anderson jr., *Phys. Rev. Lett* 55, 2103 (1985).
- [6] M. Ding, C. Grebogi and E. Ott, *Phys. Rev* A39, 2593 (1989); M. Ding and J.A. Scott Kelso, *Int. J. Bifurcation and Chaos* 4, 553 (1994).
- [7] J. F. Heagy and W.L. Ditto, *J. Nonlinear Sci* 1, 423 (1991).
- [8] J.I. Staglino, J.M. Wersinger, E.E. Slaminka, *Physica* D92, 164 (1996).
- [9] T. Yalinkaya and Y. C. Lai, *Phys. Rev. Lett.* 77, 5040 (1996).
- [10] T. Kapitaniak and J. Wojewoda, *Attractors of Quasiperiodically Forced Systems*, (World Scientific, Singapore, 1993).
- [11] A. Venkatesan and M. Lakshmanan, *Phys. Rev* E55, 4140 (1997).
- [12] Z. Zhu and Z. Liu, *Int. J. Bifurcation and Chaos* 7, 227 (1997).
- [13] T. Kapitaniak and L. O. Chua, *Int. J. Bifurcation and Chaos* 7, 423 (1997).
- [14] J. F. Heagy and S. M. Hammel, *Physica* 70D, 140 (1994).
- [15] A. S. Pikovsky and U. Feudel, *J. Phys.* A27, 5209 (1994).
- [16] A. S. Pikovsky and U. Feudel, *Chaos* 5, 253 (1995).
- [17] U. Feudel, J. Kurths and A.S. Pikovsky, *Physica* 88D, 176 (1995).
- [18] S. P. Kuznetsov, A.S. Pikovsky and U. Feudel, *Phys. Rev.* E51, R1629 (1995).
- [19] T. Kapitaniak, *Phys. Rev.* E47, 1408 (1993).
- [20] V.S. Anishchensko, T.K. Vadivasova, and O. Sosnovtseva, *Phys. Rev. E* 53, 4451 (1996).
- [21] T. Nishikawa and K. Kaneko, *Phys. Rev.* E54, 6114 (1996).
- [22] O. Sosnovtseva, U. Feudel, J. Kurths and A. Pikovsky, *Phys. Lett* A218, 255 (1996).
- [23] W. L. Ditto, M. L. Spano, H.T. Savage, S.N. Rauseo, J.F. Heagy and E.Ott, *Phys. Rev. Lett* 65, 533 (1990).
- [24] T. Zhou, F. Moss and A. Bulsara *Phys. Rev.* A45, 5394 (1992).
- [25] W.X. Ding, H. Deutsch, A. Dingklage and C. Wilke, *Phys. Rev.* E55, 3769 (1997).
- [26] P. Grassberger and I. Procaccia, *Phys. Rev. Lett.* 50, 346 (1983).
- [27] A. H. Nayfeh and D. T. Mook, *Nonlinear Oscillations*, (Wiley Interscience, New York, 1995).
- [28] M. Bier and T.C. Bountis, *Phys. Lett.* A104,239 (1984).
- [29] M. Lakshmanan and K. Murali, *Chaos in Nonlinear Oscillators: Controlling and Synchronization*, (World Scientific, Singapore, 1996).

TABLES

TABLE I. Characteristics of attractors

Types of attractors	Winding number	Lyapunov exponents	Power law relations	Dimensions
three frequency quasiperiodic	$W \neq \frac{m}{n}\omega_p + \frac{l}{n}\omega_e$	$\lambda_1 < 0, \lambda_2 = \lambda_3 = \lambda_4 = 0$	$N(\sigma) = \ln^2 \sigma$	Integers
two frequency quasiperiodic	$W = \frac{m}{n}\omega_p + \frac{l}{n}\omega_e$	$\lambda_1, \lambda_2 < 0, \lambda_3 = \lambda_4 = 0$	$N(\sigma) = \ln \frac{1}{\sigma}$	Integers
strange nonchaotic attractor	$W \neq \frac{m}{n}\omega_p + \frac{l}{n}\omega_e$	$\lambda_1, \lambda_2 < 0, \lambda_3 = \lambda_4 = 0$	$N(\sigma) = \sigma^{-\beta}$ $1 < \beta < 2$	Fractals

FIGURES

FIG. 1. Phase diagram of the two parameters ($f - \epsilon$) space exhibited by the system (5). Regions of different attractors are denoted as: 1T - two frequency quasiperiodicity attractor, 2T- torus doubled attractor, W1- wrinkled attractor of period one, W2 - wrinkled attractor of period two, S - strange nonchaotic attractor, S2- period doubled strange nonchaotic attractor and C - chaotic attractor.

FIG. 2. Projection of the two frequency quasiperiodic attractors of Eq. (5) for $f=0.302$: Poincaré plot with $\phi \bmod 2\pi$ in the (x, ϕ) plane, (a) two frequency quasiperiodic attractor at $\epsilon=0.030$, (b) torus wrinkled attractor for $\epsilon=0.0405$, (c) strange nonchaotic attractor for $\epsilon=0.0419$, (d) chaotic attractor for $\epsilon=0.042$, The other parameters are $\omega_o^2=0.25$, $\lambda=0.5$, $\alpha=0.2$, $\omega_p=1.0$, $\Omega_o^2=6.7$ and $\omega_e=0.991$.

FIG. 3. Largest Lyapunov exponent λ_{max} vs. ϵ corresponding to fig. 2

FIG. 4. Projection of the two frequency quasiperiodic attractors of Eq. (5) for $f=0.302$: Poincaré surface of section in the (x, y) plane (a) torus at $\epsilon=0.03$, (b) torus doubled attractor at $\epsilon=0.0317$. The other parameters are $\omega_o^2=0.25$, $\lambda=0.5$, $\alpha=0.2$, $\omega_p=1.0$, $\Omega_o^2=6.7$ and $\omega_e=0.991$.

FIG. 5. Projection of the two frequency quasiperiodic attractors of Eq.(5) for $f=0.302$: Poincaré surface of section with $\phi \bmod 2\pi$ in the (x, ϕ) plane (a) two frequency quasiperiodic attractor for $\epsilon=0.03$, (b) torus doubled attractor at $\epsilon=0.0317$, (c) & (d) same as (a) & (b) except $\phi \bmod 4\pi$ during integration. The other parameters are $\omega_o^2=0.25$, $\lambda=0.5$, $\alpha=0.2$, $\omega_p=1.0$, $\Omega_o^2=6.7$ and $\omega_e=0.991$.

FIG. 6. Projection of the two frequency quasiperiodic attractors of Eq.(5) for $f=0.32$: Poincaré plot with $\phi \bmod 2\pi$ in the (x, ϕ) plane, (a) merged attractor for $\epsilon=0.0353$ (b) wrinkled attractor for $\epsilon=0.0399$ (c) strange nonchaotic attractor for $\epsilon=0.041$ (d) chaotic attractor for $\epsilon=0.0413$ The other parameters are $\omega_o^2=0.25$, $\lambda=0.5$, $\alpha=0.2$, $\omega_p=1.0$, $\Omega_o^2=6.7$ and $\omega_e=0.991$.

FIG. 7. Largest Lyapunov exponent λ_{max} vs. ϵ corresponding to Figs. 4,5 & 6

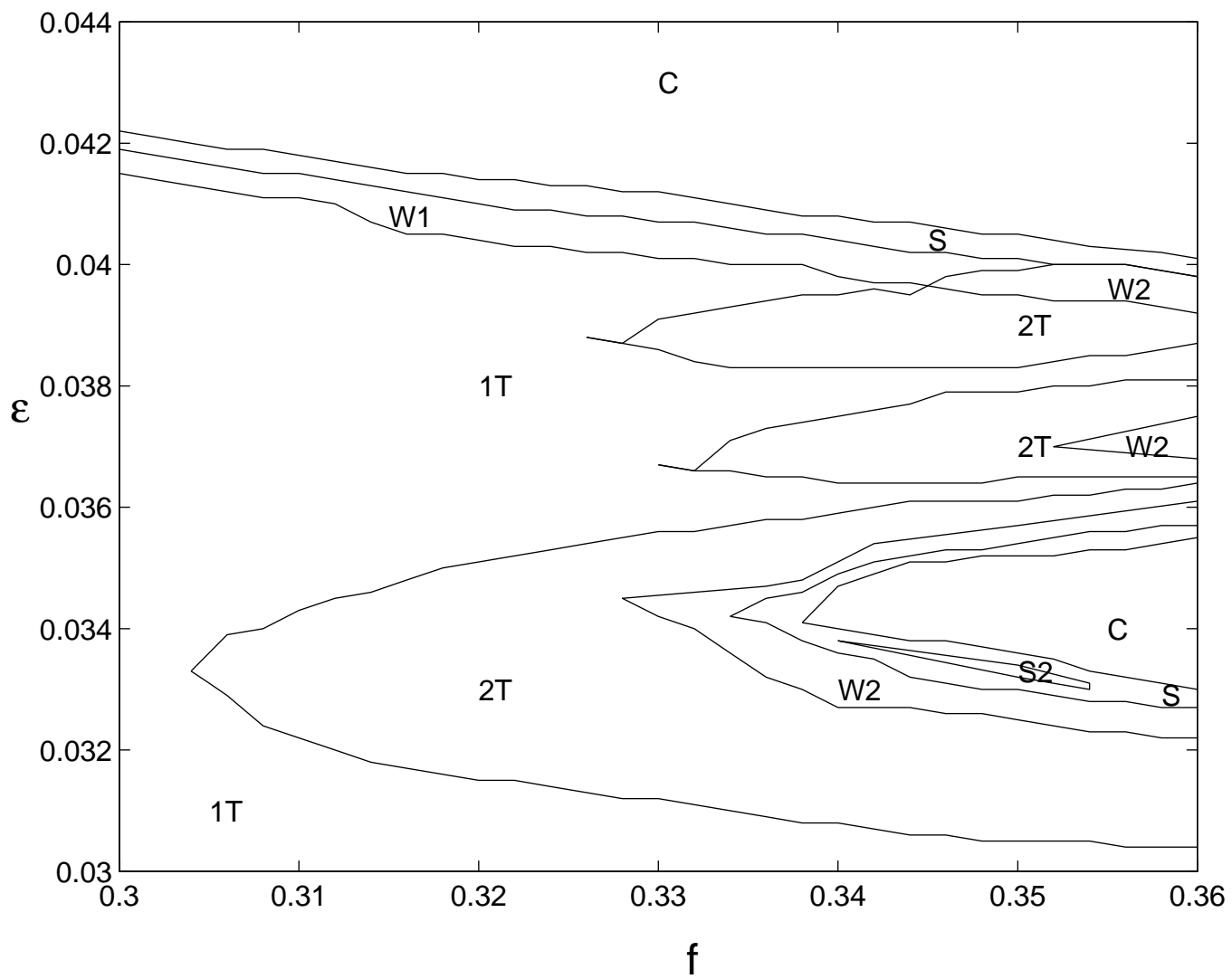
FIG. 8. Projection of the two frequency quasiperiodic attractors of Eq.(5) for $f=0.337$: Poincaré plot with $\phi \bmod 2\pi$ in the (x, ϕ) plane, (a) two frequency quasiperiodic torus at $\epsilon=0.03$, (b) doubled torus attractor for $\epsilon=0.0312$, (c) wrinkled doubled attractor for $\epsilon=0.0335$, (d) strange nonchaotic attractor for $\epsilon=0.0342$, (e) strange nonchaotic attractor for $\epsilon=0.0345$, (f) wrinkled attractor for $\epsilon=0.03461$ (g) doubled torus attractor for $\epsilon=0.0347$, (h) merged attractor for $\epsilon=0.036$, The other parameters are $\omega_o^2=0.25$, $\lambda=0.5$, $\alpha=0.2$, $\omega_p=1.0$, $\Omega_o^2=6.7$ and $\omega_e=0.991$.

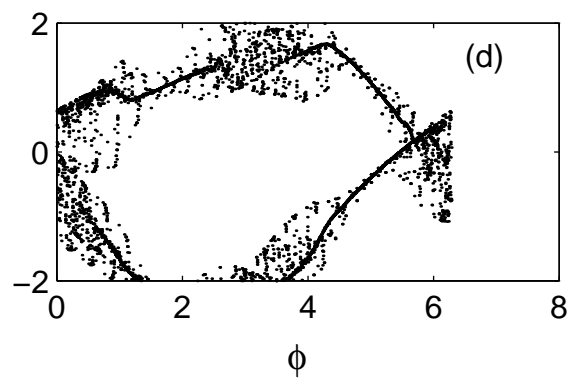
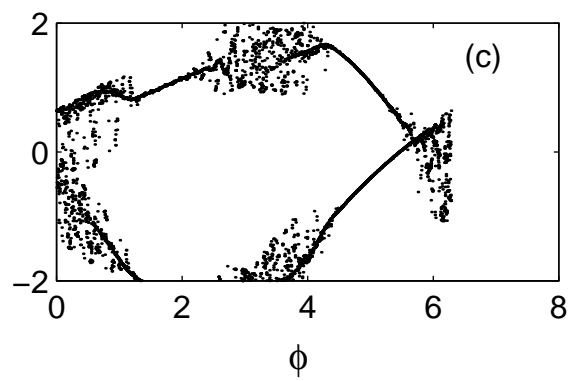
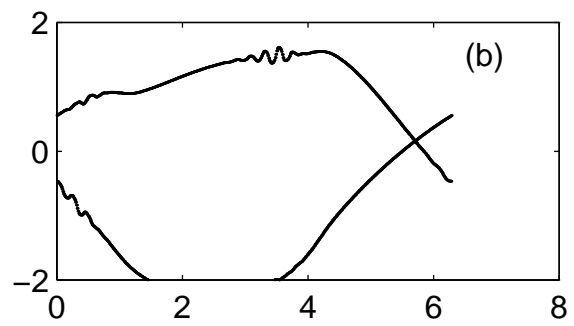
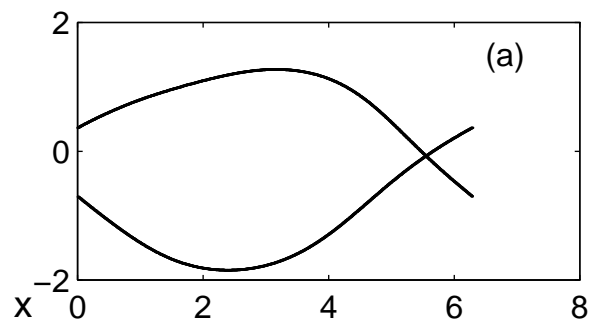
FIG. 9. Largest Lyapunov exponent λ_{max} vs. ϵ corresponding to Fig.8

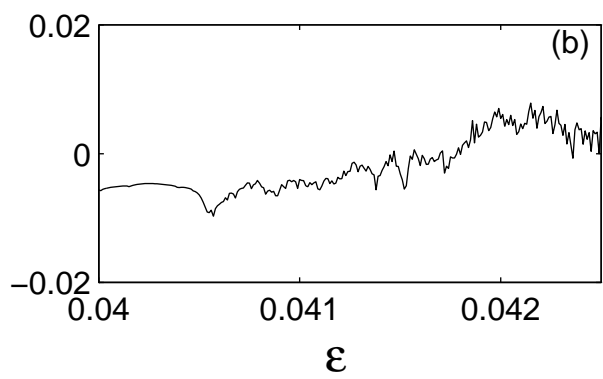
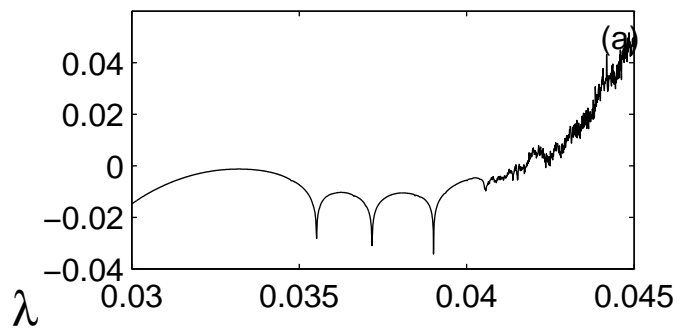
FIG. 10. Projection of the two frequency quasiperiodic attractors of Eq.(5) for $f=0.342$: Poincaré plot with $\phi \bmod 2\pi$ in the (x,ϕ) plane, (a) two frequency quasiperiodic torus at $\epsilon=0.03$, (b) doubled torus attractor for $\epsilon=0.0309$, (c) wrinkled doubled attractor for $\epsilon=0.033$, (d) strange nonchaotic attractor for $\epsilon=0.0337$, (e) chaotic attractor for $\epsilon=0.034$, (f) strange nonchaotic attractor for $\epsilon=0.0345$, (g) doubled torus attractor for $\epsilon=0.0347$, (h) merged attractor for $\epsilon=0.036$, The other parameters are $\omega_o^2=0.25$, $\lambda=0.5$, $\alpha=0.2$, $\omega_p=1.0$, $\Omega_o^2=6.7$ and $\omega_e=0.991$.

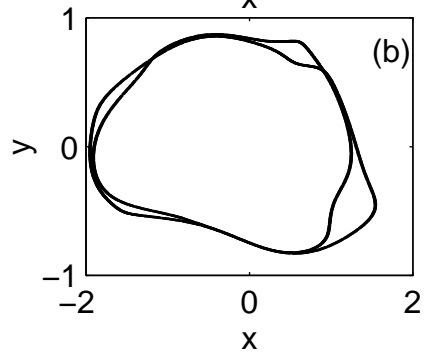
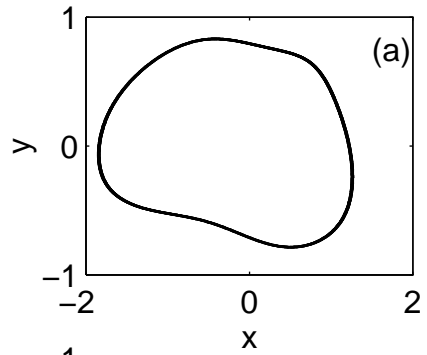
FIG. 11. Largest Lyapunov exponent λ_{max} vs. ϵ corresponding to Fig.10

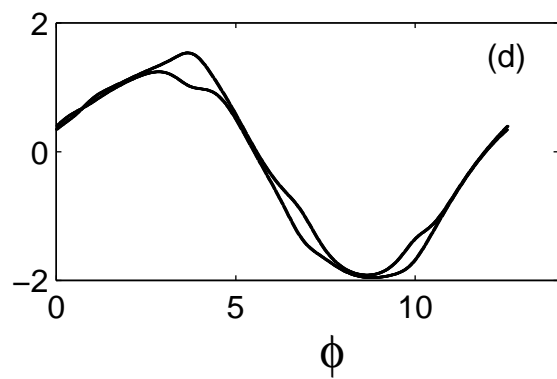
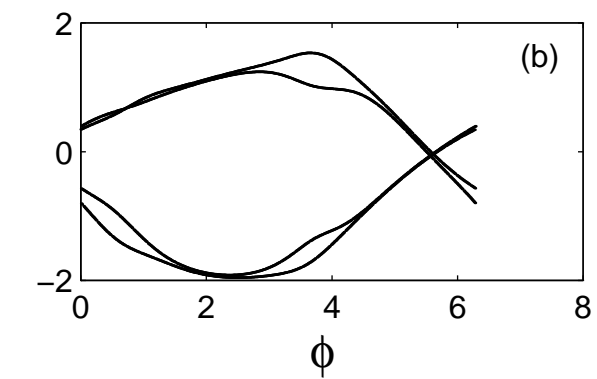
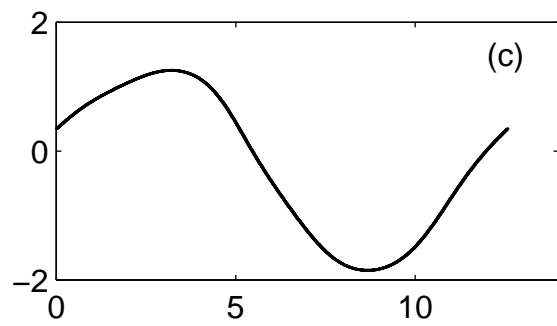
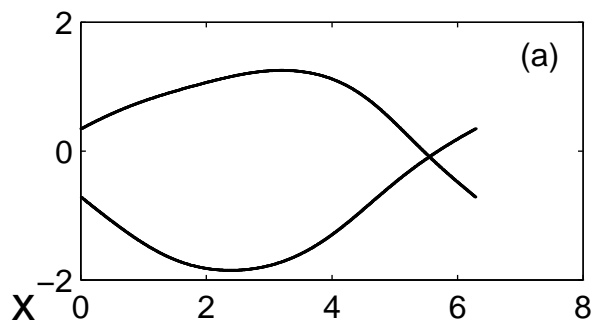
FIG. 12. Projection of the two frequency quasiperiodic attractors of Eq.(5) for $f=0.345$: Poincaré plot with $\phi \bmod 2\pi$ in the (x,ϕ) plane, (a) two frequency quasiperiodic torus at $\epsilon=0.03$, (b) doubled torus attractor for $\epsilon=0.0305$, (c) strange nonchaotic attractor for $\epsilon=0.0334$, (d) doubled strange nonchaotic attractor for $\epsilon=0.0337$, The other parameters are $\omega_o^2=0.25$, $\lambda=0.5$, $\alpha=0.2$, $\omega_p=1.0$, $\Omega_o^2=6.7$ and $\omega_e=0.991$.

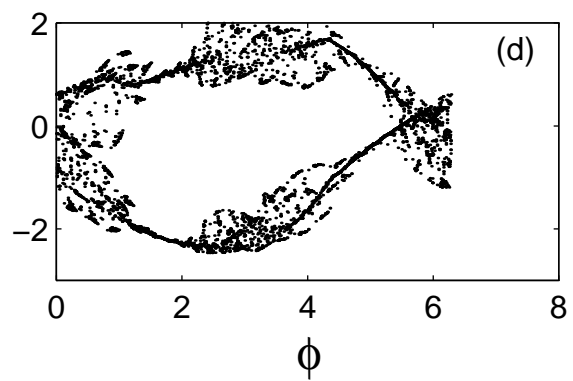
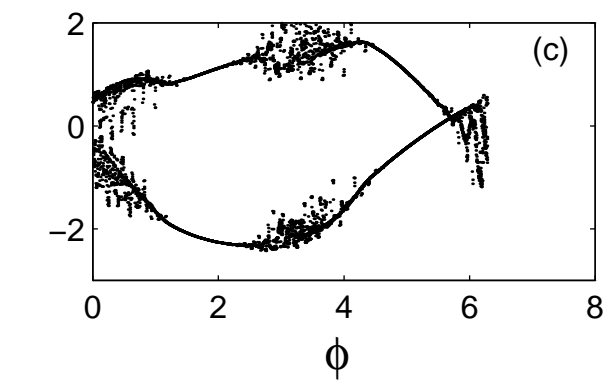
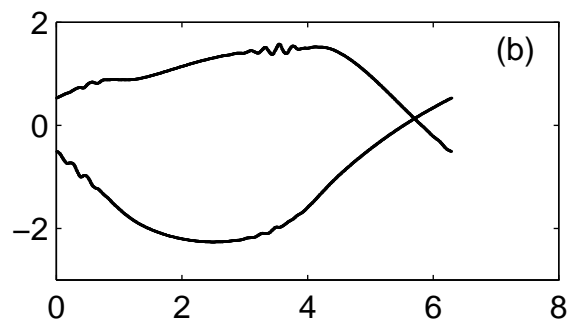
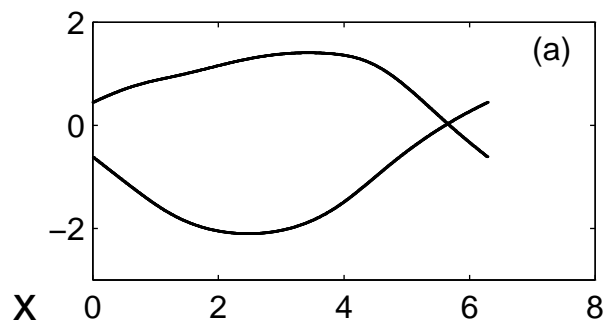


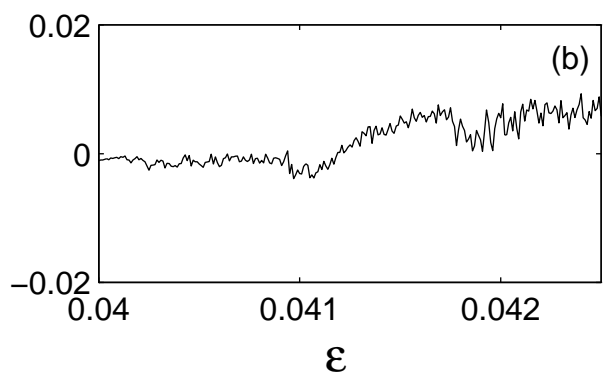
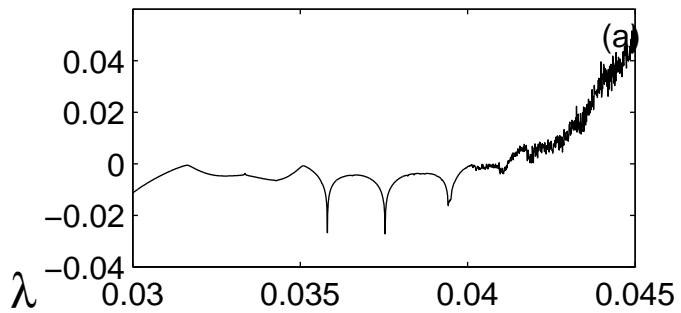


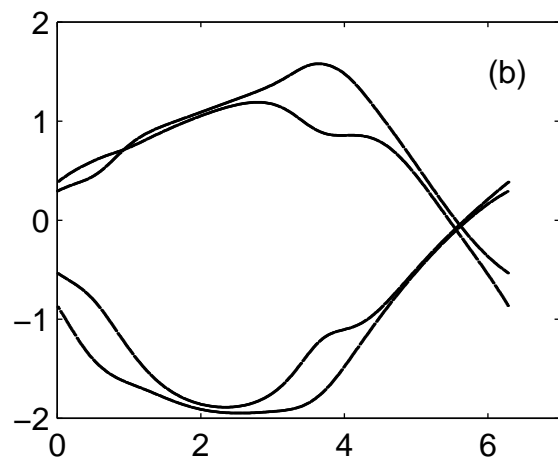
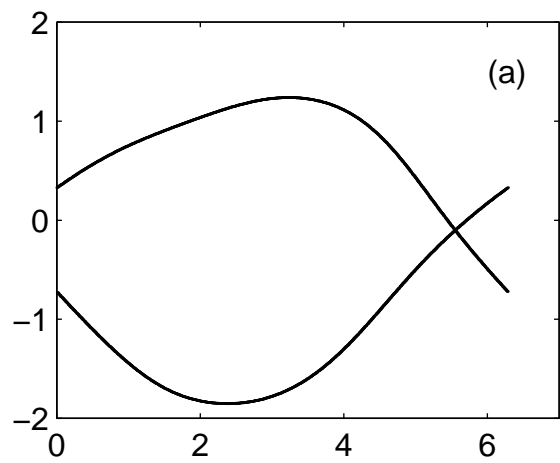




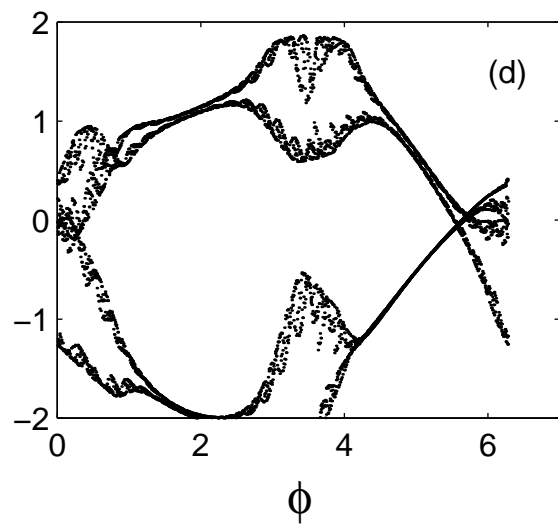
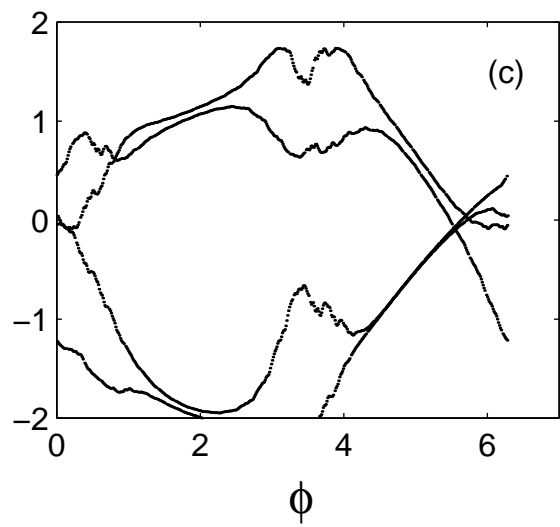


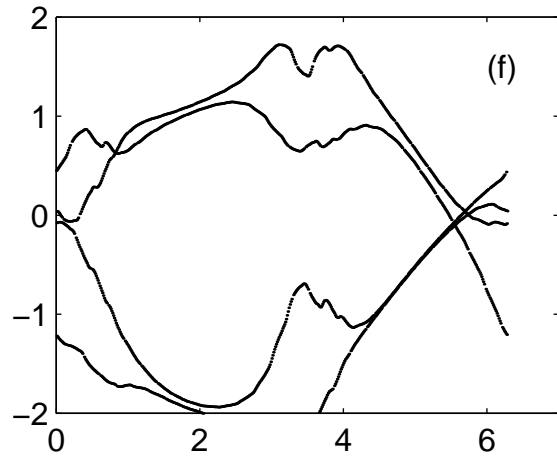
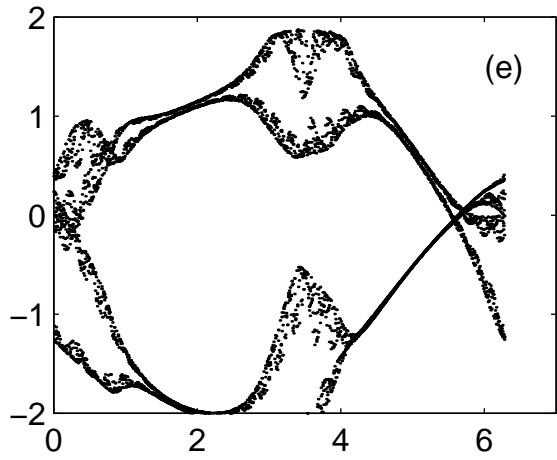




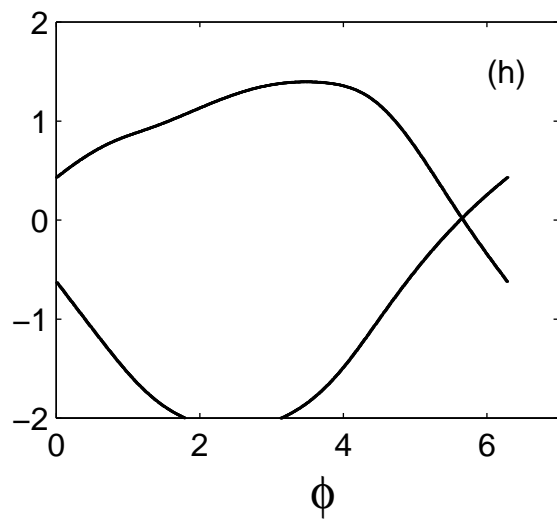
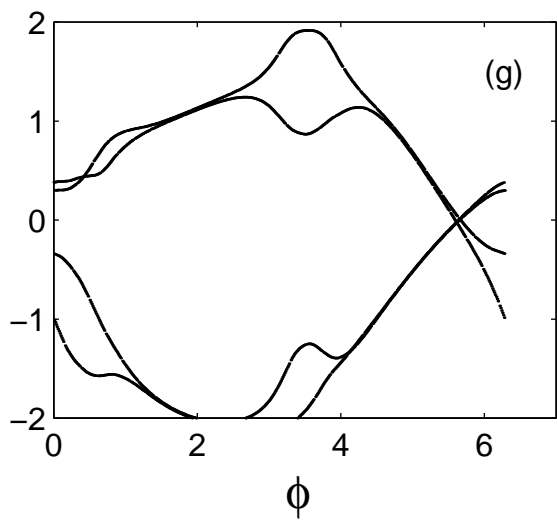


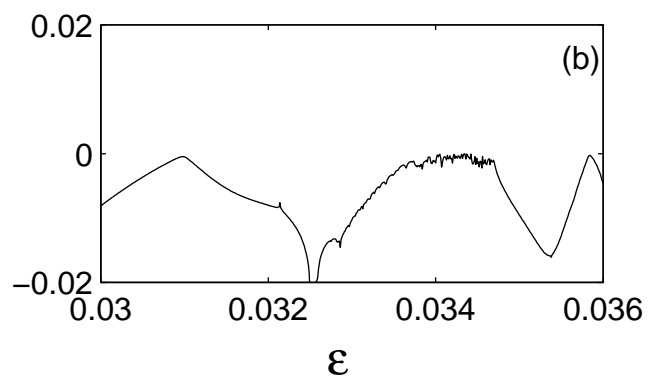
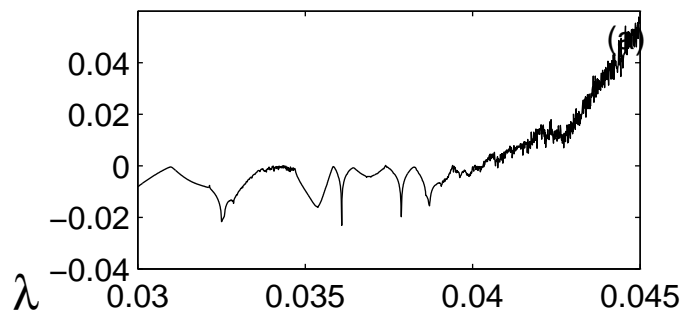
X

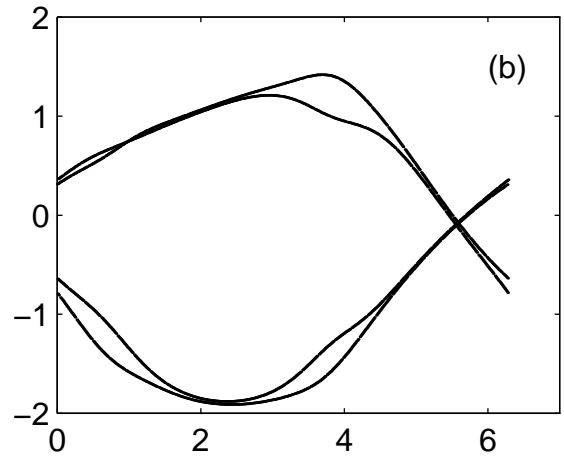
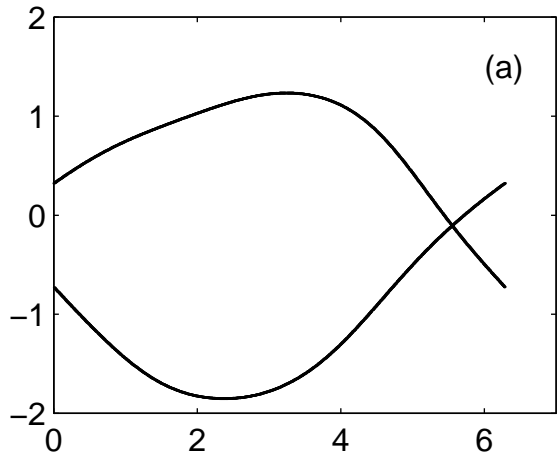




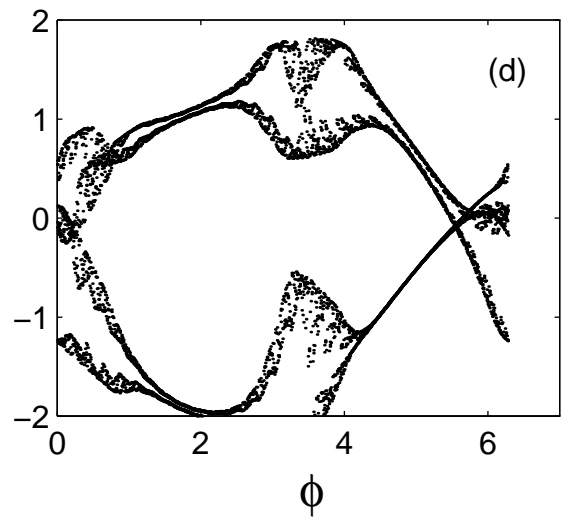
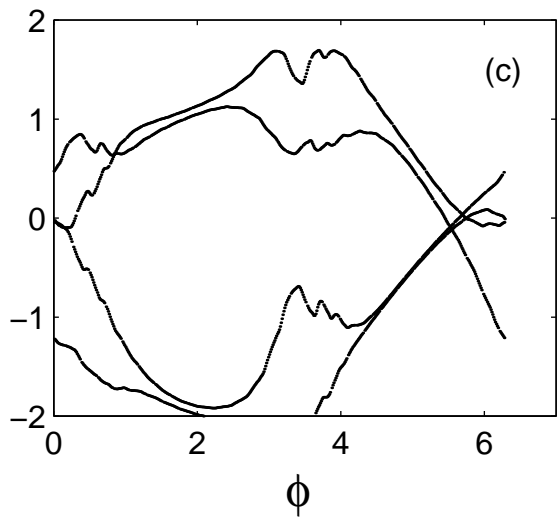
X

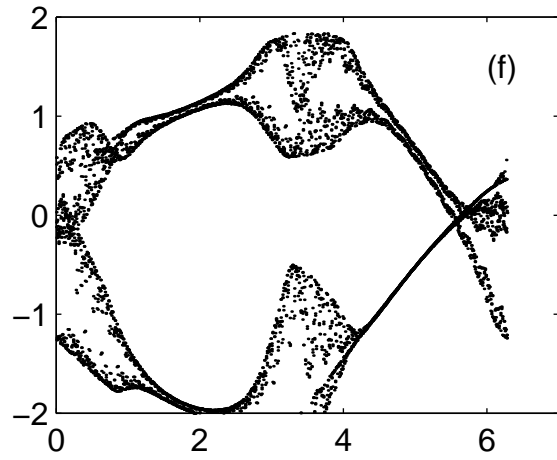
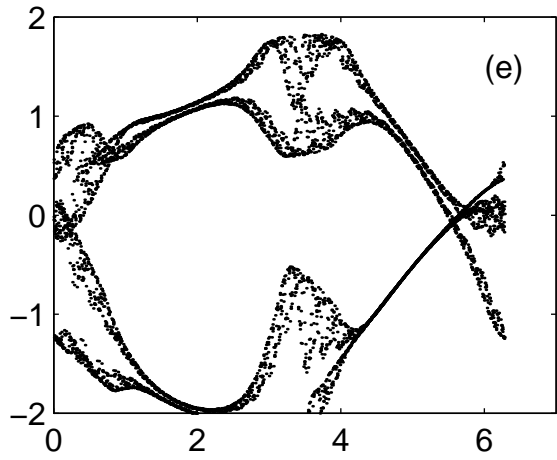






X





X

